Mar Geophys Res (2008) 29:161–165
DOI 10.1007/s11001-008-9052-y

ORIGINAL RESEARCH PAPER

Gravity effect of spreading ridges: comparison of 2D and spherical models

Hasan Çavşak

Received: 28 July 2007 / Accepted: 9 July 2008 / Published online: 31 July 2008

Abstract Because of its importance to many Earth science analyses, it is worth assessing whether gravity modelling can be simplified depending on the intended purpose and required precision. While it is obvious that large-scale gravity studies should account for the sphericity of the Earth, each case should be examined on its own merits. Demonstrations are useful for providing estimates of the errors in much simpler 2D modelling. The example of the Mid-Atlantic Ridge serves to compare "large" 2D and spherical 3D models. My model extends horizontally ±2,000 km (±18°) from the model profile across and along the straight ridge axis (along a great circle) and to a depth of 82 km across the axis. 3D modelling would generally be considered obligatory, but this is not clearly necessary from this study. The density structure is highly idealised, the asthenospheric uplift or lithosphere thinning is simplified. The Bouguer anomaly is fitted by least-squares for the density contrast, and the 2D–3D difference of the results is taken as the error. A lithosphere–asthenosphere density contrast of 86.56 kg/m^3 was computed for the 2D model, and 84.14 kg/m^3 for the spherical model. The difference is small, in the order of 3%, well within all the other uncertainties. My study shows that despite the significant sphericity of the structure, 2D models are well suited for such ridge studies, or generally for models with a laterally extended layered structure, and that spherical modelling can be applied discriminately.

Keywords 2D · Spherical gravity modelling · Ocean ridges

H. Çavşak (✉)
Geophysics Engineering Department, Karadeniz Technical University, 61080 Trabzon, Turkey
e-mail: cavsak@ktu.edu.tr

Introduction

It is usually assumed that to be done correctly gravity calculations for large-scale models must performed in 3D spherical coordinates. Appropriate algorithms have been in the literature for decades and standard routines are available (Takin and Talwani 1966; Jonson and Litehiser 1972; Talwani 1973; Vyskocil and Burda 1976; Cochran and Talwani 1978; von Frese et al. 1981). Nonetheless, this author has also used his own 3D routine (Çavşak 1992). Obviously, the meaning of "large scale" depends on the problem and the special requirements of each project. Moreover, 3D models are much more difficult to work with, to assess and evaluate, so that it is worth considering the much easier and more manageable 2D models whenever possible. The present study is motivated by a 2D Cartesian study by Jacoby and Çavşak (2005) who, for simplicity, compared oceanic ridge systems by applying 2D models of several thousand kilometres extent. However, geometrically a surface point P, 10° removed from the observation O, lies nearly 100 km below the plane level through O, which will in turn affect the gravity effect. In spite of this, no quantitative estimate of the errors due to 2D modelling and of the validity of the comparison were offered by Jacoby and Çavşak (2005).

Here, I present a simple test for such ocean ridge models using a very simple model, the lithosphere–asthenosphere structure being described by an upward pointing low-density wedge as was also partly used by Jacoby and Çavşak (2005). This approach defines the lithosphere on the basis of thermal models and particularly the 1,300°C isotherm (Artemieva and Mooney 2002). The depth extent of about 80 km is considered to be realistic for the test performed here. The effects of a 2D wedge are compared to those calculated for a spherical model of such a wedge in a quadrangle of about

18° × 18° or 4,000 × 4,000 km area; the ridge follows the centre line of the quadrangle and the gravity profile is the perpendicular centre line (Fig. 1). The method of comparison, 2D—spherical, is a simple linear inversion for the best-fitting density, given the average Bouguer anomaly across the Mid-Atlantic Ridge. While the 2D ridge structures in the study mentioned were more complex, the present test gives an instructive quantification of the differences to be expected between 2D and spherical models (Fig. 1).

Model and data

For the 2D gravity calculations a 4,000-km-long lithosphere–asthenosphere section in the x-direction was assumed to extend 2,000 km on either side of the ridge crest (Fig. 2). The upper surface is planar, and the water–lithosphere boundary is computationally removed by the Bouguer reduction with a Bouguer density of 1,600 kg/m^3 (rock–water). The upper surface of the asthenospheric wedge is approximated by a polygon, and the horizontal lower surface is, again, assumed to be a straight line in Cartesian coordinates. The lithosphere reaches a maximum thickness of 82 km at 2,000 km axial distance. The base of the lithosphere corresponds roughly to the definition of the 1,300°C isotherm (Artemieva and Mooney 2002) and is considered adequate for this test. This simplistic model of the depth structure of the ridge is adapted from a mean section of the Mid-Atlantic Ridge (Jacoby and Çavşak 2005). More detailed and realistic models of cooling lithosphere and crust-mantle structure are immaterial for the present test. What is important here is the ratio of depth over lateral extent of the model.

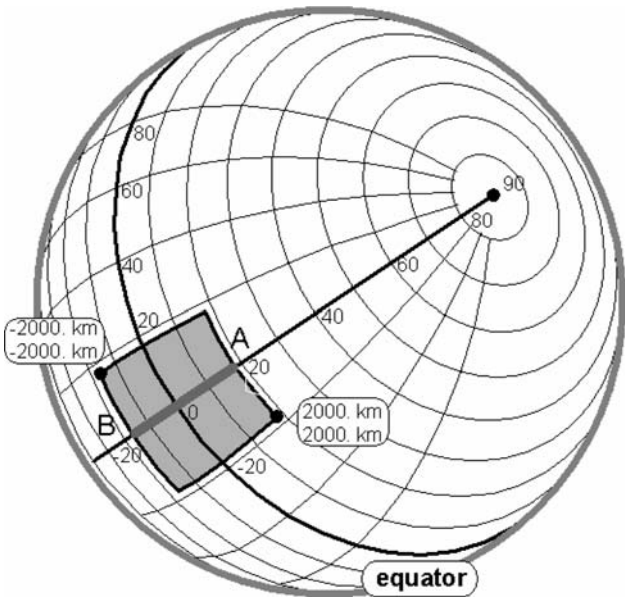

Fig. 1 The spherical model quadrangle

The spherical 3D model has the same 2D section transferred into the quadrangle of the spherical Earth, as shown in Fig. 1. The ridge is assumed to be perpendicular to the equator, along a meridian. For the gravity calculation, the cross section is defined in spherical coordinates extending to ±18°, i.e. ±2,000 km along the Earth's surface. The 3D model is represented by nine sub-parallel cross sections along parallels, 4.5° or 500 km apart, each defined by 43 polygonal corner points, and connected by triangulation to form upper and lower polyhedral surfaces of the asthenosphere wedge, thus defined by 1,508 triangles. Figure 3 shows the model geometry in spherical form.

The comparison between Cartesian 2D and spherical 3D modelling is made on the basis of observational data from the Mid-Atlantic Ridge. On the basis of the global

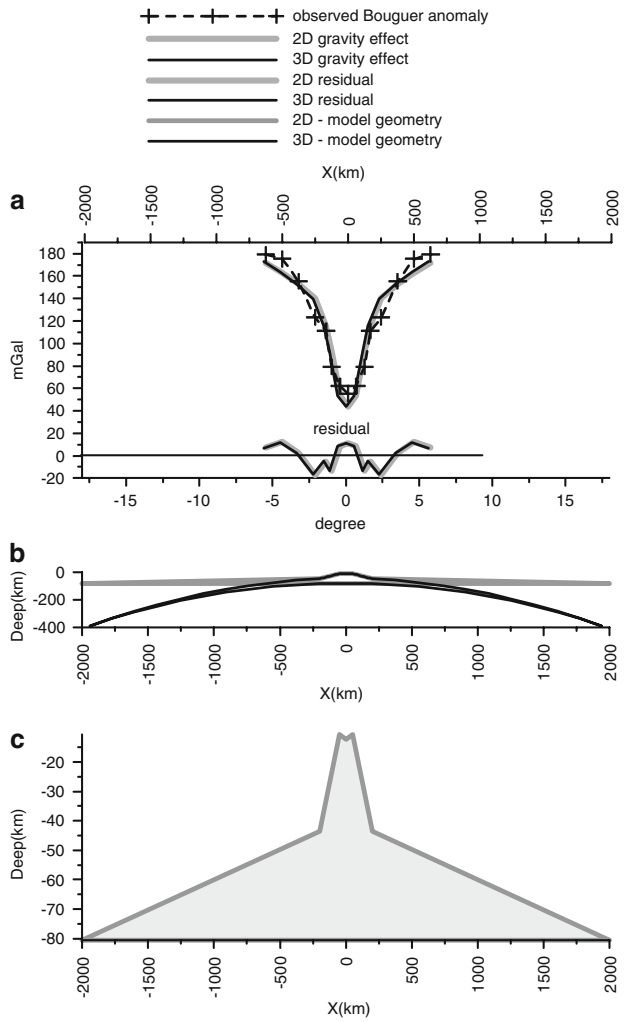

Fig. 2 (**a**) Mean observed Bouguer anomaly across the Mid-Atlantic ridge and gravity effects calculated for the Cartesian 2D model and for the spherical 3D model. (**b**) Cross section of the assumed asthenosphere–lithosphere structure in the 2D and spherical 3D coordinates. (**c**) The vertically exaggerated section (25x) shows the slight axial depression

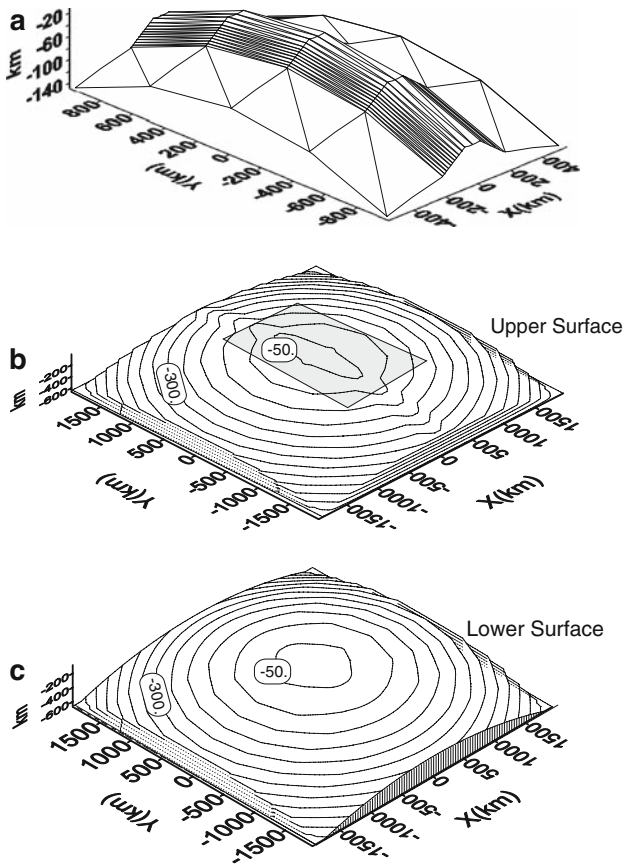

Fig. 3 (**a**) 2D Upper surface. (**b**) and (**c**) Upper and lower surface of the body in the geographical coordinates, defined with 43 × 9 corner points and contoured in 50-km depth intervals relative to the centre point at the earth's surface; bottom: the lower surface of the low-density asthenosphere wedge; middle: the top surface of the asthenosphere wedge; top: a central section shown in the middle by grey shading

spherical harmonic gravity field solution of Rapp (1977), which is complete to degree and order 52, profiles were selected that are as little as possible disturbed by fracture zones and seamounts (Fischer 1984; Vesper 1984) and then stacked to obtain a representative "average profile". The selected data points are shown as crosses in Fig. 2, together with the modelling results. Bathymetry was taken from a global data set of 1° × 1° mean values (R. Rummel, personal communication) and is treated in exactly the same way as gravity. For the 2D–3D comparison, the data are considered sufficient and adequate for the demands of this particular exercise.

Results

For the comparison of 2D and 3D gravity models, an inversion of the Bouguer anomaly data set was carried out using the two model types as a priori information. Only the density contrast between the thickening lithosphere and the wedge-shaped asthenosphere was adjustable. That does not mean that such a model is considered most realistic, but it can be taken as an "equivalent" model in the sense that it can explain the main features of the observed Bouguer gravity anomaly. Geological complications and details are intentionally neglected. Undoubtedly, they would affect the comparison slightly, but the main effect of global geometry, i.e. spherical versus 2D, should be rather accurately quantified and not affected by this simplification. Table 1 gives the details of fitting both models.

The best-fitting density contrasts are taken as an indication of the errors encountered in 2D modelling. The results for the two models are:

Cartesian 2D model: $\delta\rho = 86.56 \pm 5.9$ kg/m^3, standard fitting error of ±11.5 mGal,

spherical model: $\delta\rho = 84.14 \pm 5.5$ kg/m^3, standard fitting error of ±11.1 mGal.

The difference of 2.4 kg/m^3 is within the standard errors, and corresponds to less than 3% of the result. This value is rather insignificant in view of the simplifications and all the other uncertainties of such calculations.

Interestingly, the standard error of the 3D model fit is a little smaller than that of the 2D model fit. A value of 11–12 mGal reflects the shorter-scale variations for which the parametrization of the models, both 2D and spherical, is insufficient, i.e. which cannot, and were not intended to, be fitted. But the model-wide wavelength is slightly better fitted in spherical geometry.

The test was extended to the depth extent of the model by simply stretching the lithosphere–asthenosphere boundary downward and repeating the above comparison. Somewhat surprisingly, the optimised density contrasts of the 2D and 3D models diverged much less than expected as the model depths increased. The reason for this is that the structure type investigated is of layered nature, with a lateral extent greatly exceeding its depth. The problems of 2D models become serious, when the vertical dimensions approach the model width, as in the case of narrow mantle plumes.

Discussion

This study was suggested by modelling of several ocean ridges by Jacoby and Çavşak (2005). This earlier study left open the question of how large the errors in 2D versus 3D models had been. Here, I used a simple model to show that the systematic error in the 2D models caused by ignoring the real 3D spherical geometry is only small, i.e. a fraction of the standard error of the fit to the data. The resultant error is a slight overestimation of the density contrast between lithosphere and asthenosphere. In the case of a ridge with 4,000 km lateral dimensions and a depth extent of the order of 100 km, 2D modelling is still adequate for a

Table 1 Observed Bouguer anomaly and calculated gravity effect of ridge Model and residuals for 2D Cartesian model and 3D spherical model

X (km)	Observed (mGal)	2D		3D	
		Calculated (mGal)	Residual (mGal)	Calculated (mGal)	Residual (mGal)
−625.00	**179.00**	**171.82**	**7.18**	**172.43**	**6.57**
−500.00	175.00	162.65	12.35	163.13	11.87
−375.00	155.00	152.96	2.04	152.84	2.16
−250.00	123.00	140.13	−17.13	139.76	−16.76
−168.00	111.00	116.16	−5.16	115.49	−4.49
−125.00	79.00	92.69	−13.69	92.37	−13.37
−62.00	62.00	53.21	8.79	53.48	8.52
0.00	**55.00**	**43.77**	**11.23**	**43.97**	**11.03**
62.00	62.00	53.21	8.79	53.48	8.52
125.00	79.00	92.69	−13.69	92.37	−13.37
168.00	111.00	116.16	−5.16	115.49	−4.49
250.00	123.00	140.13	−17.13	139.76	−16.76
375.00	155.00	152.96	2.04	152.84	2.16
500.00	175.00	162.65	12.35	163.13	11.87
625.00	**179.00**	**171.82**	**7.18**	**172.43**	**6.57**
Standard error: 11.48 mGal, Constant: 270.75 mGal				Standard error: 11.07 mGal, Constant: 282.20 mGal	

2D-$\Delta\rho = -86.6$ kg/m^3,
3D-$\Delta\rho = -84.5$ kg/m^3

regional study and does not require the more complex 3D approach for a realistic prediction. This conclusion still holds for deeper structures of similar "layered" geometry to depths comparable with the model widths.

Acknowledgments I thank my former advisor, Prof. Dr. Wolfgang Jacoby for his suggestions, encouragement and efforts with helping me formulate this work in English. I thank Dr Horst Holstein, from whom I have benefited through helpful discussions. I also thank Dr. Peter Clift for his suggestions. The reviewers gave further helpful criticism.

Appendix

Calculation of the potential and the gravity effect

The 2D calculations were carried out with the widely known Talwani method (Talwani et al. 1959). For the 3D calculations the program INVGRA. for was written by the first author as part of his PhD thesis (Çavşak 1992). The parametrization of arbitrarily shaped uniform mass bodies is based on triangulated polyhedra, a classical method in gravity calculations (e.g. Chapman 1979; Holstein et al. 1999; Holstein 2002a, b; Pohánka 1988). A brief outline of the method follows below as it had been derived in a non-traditional way.

Given is the terrestrial x, y, z coordinate system with z pointing downward in $\boldsymbol{g}$ direction. The basic unit of the massive polyhedron is defined by the tetrahedron expanded from the observation point O to any of the planar triangles. Their orientation is arbitrary in (x, y, z). A coordinate transformation is carried out (by vector operations) to the triangle-oriented coordinate system (ξ, η, ζ), such that the triangle is in the ξ–η plane and one of its edges (A–B) is parallel to ξ, see Fig. A-1.

The potential effect is given by

$$\Delta U = \frac{G\cdot\rho}{h}\int_{\eta_A}^{\eta_C}\int_{\xi^{(1)}}^{\xi^{(2)}}\int_{\zeta=0}^{h}\frac{\zeta\cdot d\zeta\cdot d\xi\cdot d\eta}{(\xi^2+\eta^2+h^2)^{1/2}} \tag{A-1}$$

where h is the height of tetrahedron (Fig. A-1)

Analytical integration renders $\Delta U = \frac{1}{2}G\cdot\rho\cdot h\cdot F(\eta,\xi)$ with

$$F(\eta,\xi) = \left|\begin{array}{l}\eta\cdot\ln\left[\xi+\sqrt{\xi^2+\eta^2+h^2}\right]\\ +\xi_2\cdot\cos\beta\cdot\ln\left[\sqrt{\xi^2+\eta^2+h^2}+\dfrac{\eta}{\cos\beta}+\xi_2\cdot\sin\beta\right]\\ +\zeta\cdot\arctan\left[\dfrac{h^2\cdot\tan\beta-\xi_2\cdot\eta}{h\cdot\sqrt{\xi^2+\eta^2+h^2}}\right]\end{array}\right|_{\xi^{(1)^2},\eta_A}^{\xi^{(2)^2},\eta_C} \tag{A-2}$$

(Chapman 1979), from which follows:

$$Y = F_1\left(\eta_C,\xi^{(2)}\right) - F_2\left(\eta_A,\xi^{(2)}\right) - F_3\left(\eta_C,\xi^{(1)}\right) + F_4\left(\eta_A,\xi^{(1)}\right) \tag{A-3}$$

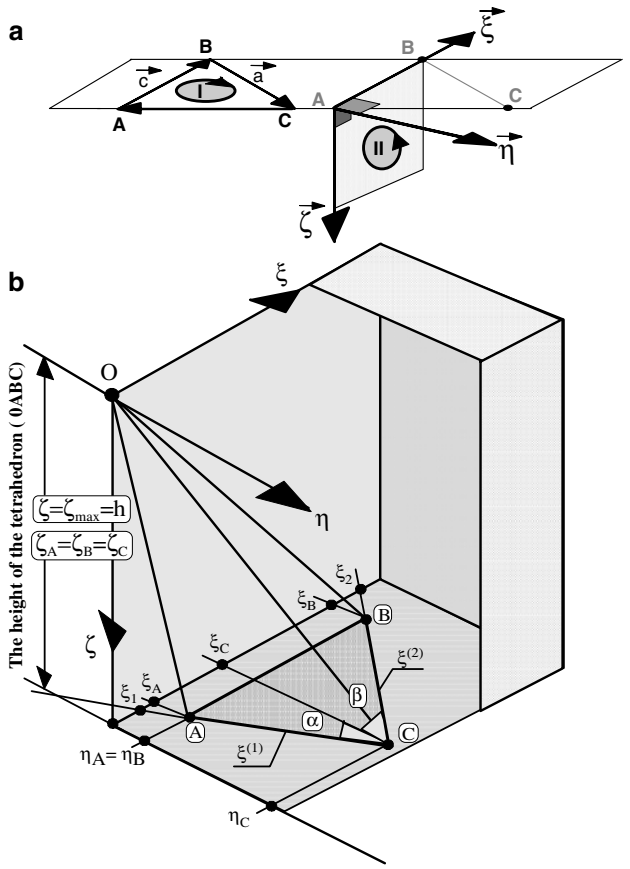

Fig. A-1 (**a**) Coordinate transformation with vector operation. (**I**) $\vec{\zeta} = \vec{c} \times \vec{a}$ and (**II**) $\vec{\eta} = \vec{\zeta} \times \vec{c}$ and (**b**) illustration of the parameters. The triangle in its transformed coordinate system

The gravity effect is

$$\Delta g = \frac{\partial}{\partial z}(\Delta U) \tag{A-4}$$

The formal differentiation leads to a lengthy expression, not reproduced here. It reduces to

$$\Delta g = \frac{1}{2} G \cdot \rho \left\{ \frac{\partial}{\partial z}(h) \cdot Y + \frac{\partial}{\partial z}(Y) \cdot h \right\} \tag{A-5}$$

With the z component of the normal unit vector of the respective triangle $\hat{\zeta}_z = \frac{\partial}{\partial z}(h)$ and $Y' = \frac{\partial}{\partial z}(Y)$ we can write

$$\Delta g = \frac{1}{2} G \cdot \rho \cdot \sum_{i=1}^{n} \left(\hat{\zeta}_{z_i} \cdot Y_i + Y_i' \cdot h_i \right) \tag{A-6}$$

References

Artemieva IM, Mooney WD (2002) Thermal thickness and evolution of Precembrian lithosphere: a global study. J Geophys Res 106:16387–16416. doi:10.1029/2000JB900439

Çavşak H (1992) Dichtemodelle für den mitteleuropäischen Abschnitt der EGT aufgrund der gemeinsamen Inversion von Geoid, Schwere und refraktionsseismisch ermittelter Krustenstruktur (in German: Density models for the central European Section of EGT on the basis of joint inversion of geoid, gravity and refraction seismic crustal structure). Ph.D. Thesis, Mainz University

Chapman ME (1979) Techniques for interpretation of geoid anomalies. J Geophys Res 84:3793–3801. doi:10.1029/JB084iB08p03793

Cochran JR, Talwani M (1978) Gravity anomalies, regional elevation, and the deep structure of the North Atlantic. J Geophys Res 83:4907–4924. doi:10.1029/JB083iB10p04907

Fischer HJ (1984) Erfassung der Schwereanomalie über ozeanischen Rücken und ihre Deutung. Diploma thesis, Geophys, Frankfurt

Holstein H (2002a) Gravimagnetic similarity in anomaly formulas for uniform polyhedra. Geophysics 67:1126–1133. doi:10.1190/1.1500373

Holstein H (2002b) Invariance in gravimagnetic anomaly formulas for uniform polyhedra. Geophysics 67:1134–1137. doi:10.1190/1.1500374

Holstein H, Schürholz P, Starr AJ, Charkraborty M (1999) Comparison of gravimetric formulas for uniform polyhedra. Geophysics 64:1438–1446. doi:10.1190/1.1444648

Jacoby WR, Çavşak H (2005) Inversion of gravity anomalies over spreading oceanic ridges. J Geodyn 39:461–474. doi:10.1016/j.jog.2005.04.011

Jonson LR, Litehiser JJ (1972) A method for computing the gravitational attraction of three-dimensional bodies in a spherical or ellipsoidal Earth. J Geophys Res 77:6999–7009. doi:10.1029/JB077i035p06999

Pohánka V (1988) Optimum expression for computation of the gravity field of a homogeneous polyhedral body. Geophys Prospect 36:733–751. doi:10.1111/j.1365-2478.1988.tb02190.x

Rapp RH (1977) Potential Coefficient Determination from Terrestrial Gravity Data. Rep. Dept. Geodetic Science, 251, Ohio State University, 1977

Takin M, Talwani M (1966) Rapid computation of the gravitation attraction of topography on a spherical Earth. Geophys Prospect 14:119–142. doi:10.1111/j.1365-2478.1966.tb01750.x

Talwani M (1973) Computer usage in the computation of gravity anomalies. In: Methods in computational physics, vol 13. Academic Press, New York, NY, pp 343–389

Talwani M, Lamar WJ, Landisman M (1959) Rapid gravity computations for two-dimensional bodies with application to the Mendocino submarine fracture zone. J Geophys Res 64(1), 49–59, 1

Vesper H (1984) Erfassung von Schwereanomalien über ozeanischen Rücken und ihre Deutung. Diploma thesis, Geophys, Frankfurt

von Frese RRB, Hinze WJ, Braile LW, Luca AJ (1981) Spherical Earth gravity and magnetic anomaly modeling by Gauss–Legendre quadrature integration. J Geophys 49:234–242

Vyskocil V, Burda M (1976) On the computation of the gravitational effect of three-dimensional density models of the Earth's crust. Stud Geophys Geod 3:213–218. doi:10.1007/BF01601900